American Journal of Engineering and Applied Sciences

Original Research Paper

A Novel Prototype of a Small-Scale Solar Power Plant: Dynamic Simulation and Thermoeconomic Analysis

Annamaria Buonomano, Francesco Calise and Maria Vicidomini

University of Naples Federico II (DII), Naples, Italy

Article history
Received: 21-11-2015
Revised: 26-11-2015
Accepted: 29-01-2016

Corresponding Author:
Francesco Calise
University of Naples Federico II (DII), Naples, Italy
Email: frcalise@unina.it

Abstract: The paper presents an innovative prototype of a solar power plant, purposely designed for small-scale applications such as residential and/or small commercial buildings. The system consists of 10 kW_e Organic Rankine Cycle (ORC) plant and innovative solar thermal collectors. In particular, 235 m^2 of flat-plate evacuated solar collectors are designed to heat diathermic oil up to 180°C. A variable volume pump is managed by a feedback controller in order to obtain the desired outlet set point temperature for the different weather/load conditions. The hot diathermic oil passes through a storage tank, which is adopted with the purpose to reduce the oscillations due to the solar radiation variability. By means of the tank, a better exploitation of solar energy is also achieved, reducing the time-shift between production and demand. For achieving a constant ORC inlet temperature the tank outlet hot diathermic oil passes through a gas-fired burner, which provides auxiliary additional thermal energy. Therefore, the ORC simultaneously produces electrical energy and low temperature (45°C) cogeneration heat. This solar power plant was dynamically simulated in TRNSYS environment. The simulation tool includes a novel model in order to simulate the dynamic thermal behavior of solar collectors, whereas the ORC dynamic was simulated by means of a performance data map provided by the manufacturer. The model also includes a tool for the calculation of energy and economic parameters and the evaluation of the optimum thermoeconomic configuration. Results indicated that the best pay-back period is obtained for a solar field area of about 200 m^2 and a solar fraction of about 75%. Nevertheless, the system may be competitive from the economic point of view only if incentives can be made available, as commonly occurs for renewable applications, i.e., solar systems. This prototypal system aims to become a potential solar power system for small residential and/or commercial buildings. The presented study will be suitably used as a basis for the installation of a working prototype in located Naples, Italy.

Keywords: Solar Energy, Organic Rankine Cycle, Dynamic Simulation

Introduction

In the last decades, the remarkable consumption of fossil fuels determined severe issues concerning their future availability. As a consequence, a significant research effort has been performed in order to investigate alternative energy sources such as renewables. In particular, several researchers focused their effort on the design and development of economically-viable technologies based on low-temperature heat sources. In this framework, special attention has been paid to develop distributed renewable power systems (solar power, photovoltaic, mini-wind, etc.) easily integrated in buildings (mainly residential and/or commercial) envelopes (typically roofs). Furthermore, in many countries, liberal policies determined the electric market deregulation, with the scope to reduce prices, support customers and promote distributed power generation. Among these innovative systems, the Organic Rankine Cycles (ORC) is commonly considered one of the most

promising technologies for its capability to convert into electricity low-temperature thermal energy such as renewables (solar energy, geothermal energy, etc.) or thermal energy cascades (Tchanche *et al*., 2011). In particular, an ORC is particularly interesting if coupled to solar energy in solar power systems.

In fact, such solar power systems may be manufactured at very low capacities, suitable for small-scale applications such as residential, offices and others (Kane *et al*., 2003). Such systems are especially attractive for isolated regions (Pikra *et al*., 2013). Usually, the small size solar power systems are coupled to concentrating solar collectors and ORC with volumetric expanders (Hoffschmidt *et al*., 2012; Kane *et al*., 2003). In power plants, the most common thermodynamic cycle is based on steam/water Rankine Cycle.

Anyway, the utilization of water as working fluid is not feasible (due to its saturation curve) when the heat source temperature is low. In such circumstance, the organic fluids show a considerably better performance than water due to higher molecular weight, lower evaporation heat, positive slope of the saturated vapour curve in the T-s diagram and lower critical and boiling temperatures (Quoilin *et al*., 2013; 2011). For such properties ORC technology is very interesting when low and medium thermal levels (solar energy, geothermal energy, biomass products, waste heat, etc.) are taken into consideration. This is presented by numerous papers available in literature, focused on the analysis of existing and potential ORC power plants, as well reviewed in reference (Tchanche *et al*., 2011). In the design of ORC power plants, the working fluid has a significant role. As a result, several carried out studies focus on the organic fluid selection criteria (Bu *et al*., 2013; Dai *et al*., 2009; Hung *et al*., 2010; Kuo *et al*., 2011; Madhawa Hettiarachchi *et al*., 2007; Rayegan and Tao, 2011; Saleh *et al*., 2007; Yamamoto *et al*., 2001). Calise *et al*. (2013a) analysed the performance of an ORC system, the same adopted for the presented work,

In this study different organic fluids and thermal source temperature level (from 120 to 300°C) were detected.

The authors results show that n-Butane and Isobutane are appropriate for the exploitation from low to high temperature heat sources, whilst when the temperature of the available thermal source reaches up to 170°C, the use ofR245fa is indicated.

As mentioned before, the majority of the studies available in literature, focused on different configurations of solar power plants based on the ORC technology, include the adoption of medium-temperature concentrating solar collectors, such as: Parabolic Trough Collectors (PTC), Fresnel and others.

Al-Sulaiman and Fahad (2014; Al-Sulaiman *et al*., 2011; 2012) investigated the exergy and energy aspects of a novel trigeneration plant including PTC, ORC and an absorption chiller. The authors results show that for the only solar mode the trigeneration exergy efficiency is maximum and equal to 20%, for the solar and storage mode is 8% and for the only storage mode is 7%.

In addition, the author concluded that the main cause of exergy destruction rate are the evaporator of ORC system and solar thermal collectors.

For this reason, in order to reduce the exergy destructed and increase the exergy efficiency of the plant, accurate selection and design of both these components is pivotal (Al-Sulaiman and Fahad, 2014; Al-Sulaiman *et al*., 2011; 2012).

Transient energy simulations for an Organic Rankine Cycle coupled to usual parabolic trough solar thermal power generation system (PT-SEGS–ORC) were carried out by means TRNSYS by He *et al*. (2012). In this study, the influence of main parameters on the efficiency of the System were investigated. The authors highlight that: (i) the availability of solar radiation sensitively influences the thermal storage optimal volume; (ii) the heat collecting efficiency rises sharply with oil flow rate and then reaches a constant value (He *et al*., 2012).

Astolfi *et al*. (2011) investigated an ORC system supplied by solar and geothermal energy.

Authors found out a levelized cost of electricity of 145-280 €/MWh, depending on the location of the plant, which resulted to be competitive with respect to large and stand-alone concentrating solar power plants (Astolfi *et al*., 2011). A similar study is also presented by Zhou *et al*. (2013). The combination of solar and geothermal heat sources powering ORC is also studied by Tempesti and Fiaschi (2013; Tempesti *et al*., 2012). Their studies show that R245fa allows the achievement of the lowest price of electricity production and the lowest overall cost of the CHP plant. Bruno *et al*. (2008) modelled and optimised a solar Organic Rankine Cycle for Reverse Osmosis (RO) desalination, using currently available solar thermal collectors. The system is supposed to be used for remote areas without (or with very high cost) access to the public electricity grid. The economic estimation also show that the optimised solar ORC-RO system is more profitable than an equivalent photovoltaic-RO plant (Bruno *et al*., 2008). This topic was also discussed by Delgado-Torres and García-Rodríguez (2010a) which analysed a joint use of the solar thermal powered organic Rankine cycle and the desalination technology of less energy consumption, Reverse Osmosis (RO).

In such study, twelve substances were considered as working fluids of the ORC and four different models of stationary solar collectors (flat plate collectors, compound parabolic collectors and evacuated tube collectors) were also taken into account. Results obtained for the solar regenerative Organic Rankine

Cycle (ORC) showed that, in general, the analysed dry fluids yield lower values of the unit aperture area than wet fluids with the exception of ammonia (Delgado-Torres and García-Rodríguez, 2010a; 2010b). The combination of solar collectors, ORC and desalination was also investigated by Li *et al*. (2013), introducing a novel transcritical ORC cycle. A more complex solar ORC system is proposed by Gang *et al*. (2011): The cycle is based on the Compound Parabolic Concentrator (CPC) and Organic Rankine Cycle. Two-stage collectors and heat storage units are adopted to improve heat collection efficiency. Organic fluid is preheated by Flat Plate Collectors (FPCs) before entering a higher temperature heat exchanger connected with the CPC. The two-stage heat storage units are composed of two types of Phase Change Material (PCM) with diverse melting temperatures. Simulation results show an appreciable increase in collector efficiency of the two-stage system (Gang *et al*., 2011).

In order to obtain a higher plant efficiency, Kosmadakis *et al*. (2011) integrate Concentrating Photovoltaic and Thermal solar collectors (CPVT) and ORC system. Here, the parabolic trough solar thermal collectors of the conventional solar plants based on ORC are replaced by CPVT, determining an additional electrical production. This type of plant is able to obtain an electrical efficiency of 11.83%, greater than the one of CPVT collectors (9.81%) (Kosmadakis *et al*., 2011).

Ksayer (2011) studies the heat recovery from condenser of the ORC supplied by solar energy. Ksayer highlights that the ORC plant is able to generate electricity, produce hot water and in addition an important advantage of this technology is the lower cost compared to standard plants of photovoltaic panels (Ksayer, 2011).

All the studies above cited deal with solar ORC system based on concentrating solar thermal collectors.

In fact, in order to obtain reasonable efficiencies from ORC, its driving temperature should be sufficiently high. To this purpose, concentrating high-temperature solar collectors are employed. The coupling between ORC and low-temperature solar collectors is scarcely investigated in literature. Only Wang *et al*. (2013) studied a regenerative ORC coupled with flat-plate solar thermal collectors. The results indicate that under the actual constraints, by increasing turbine inlet pressure and temperature or by lowering the turbine back pressure, an improvement of the system performance can be obtained. The parametric optimization also suggests that a higher turbine inlet temperature with saturated vapour state could enable a better system performance. In addition, compared with other working fluids, R245fa and R123 are the most suitable working fluids for the system due to their high system performance and low operation pressure. The obtained electrical efficiency varies from 4 and 6% (Wang *et al*., 2013).

As mentioned before, the main goal of this paper is the simulation and design of a small-size power plant supplied by solar energy, suitable for installation in small residential and/or commercial buildings. In addition, from the above discussed literature review, it can be observed that the vast majority of solar ORC power plants are combined to concentrating solar collectors. When flat-plate solar collectors are adopted, the efficiency may significantly decrease due to the lower driving temperature.

Nevertheless, it is worth noting that the present paper does not focus on centralized solar power production.

The purpose of this study is the analysis of small scale thermodynamic solar systems to be easily integrated in residential and/or commercial buildings. In this circumstance, the concentrating solar thermal collectors utilization in small-scale plant involves severe barriers to the development of such technologies. In fact, the buildings integration of concentrating solar thermal collectors is very difficult, particularly in densely populated zones. In addition, concentrating solar collectors show high energy conversion efficiencies only when accurately maintained. In fact, it is well known that their efficiency is principally affected by dust and tracking technology efficiency.

Therefore, in small-scale systems integrated in residential buildings, such accurate maintenance can be rarely performed. As a consequence, a dramatic degradation of their efficiency is generally expected.

In this study, this severe issue is overcome by implementing a novel system layout. In particular, the solar ORC system studied in this study consists of a novel stationary flat plate evacuated thermal collector.

The installation of such collectors is particularly simple, in fact the easy building integration is obtained like for other usual flat plate solar thermal collector used for producing space heating and domestic hot water.

The thermal efficiency of such innovative devices is greater than one obtained by concentrating collectors (Calise *et al*., 2015). Furthermore, this innovative collector does not utilize any system of tracking and is not very affected by dust. In authors' knowledge, this is the first analysis of high temperature non-concentrating solar thermal collectors driving ORC cycles (no similar study is available in literature).

The ORC solar power plant analysed in this study is mainly appropriate in small-scale residential areas.

Finally, the paper shows the dynamic model of such plant which, in the near future, will be experimented in Naples (South of Italy).

System Layout

The solar ORC power plant layout is depicted in Fig. 1. Here, four basic loops are shown:

- SCF: Solar Collector Fluid, consisting of diathermic oil flowing between the thermal storage tank and the solar collectors
- HF: Hot Fluid, consisting of diathermic oil flowing between the ORC evaporator and thermal storage tank
- DHW: Domestic Hot Water, consisting of produced domestic hot water by heat exchanger HE
- HW: Hot Water, consisting of hot water flowing between the ORC condenser to the users

Then, the plant consists of such principal elements:

- ORC, Organic Rankine Cycle: A 10 kW_e plant which uses R245fa as fluid, also equipped with thermal recovery at the condenser
- SC, Solar Collectors: Flat plate evacuated solar thermal collectors
- TK, Tank: A stratified thermal storage tank
- P1: A pump at fixed speed for the HF circuit
- P2: A pump at variable speed for the SCF circuit
- P3: A pump at fixed speed for the HW circuit
- HE: Heat Exchanger with Plate-Fin
- AH, Auxiliary Heater: A gas fired boiler

The plant includes numerous diverters, mixers and valves, that during time operation, are managed by a control system. The principle of operating for the investigated plant and its control strategy is explained as follows.

The solar loop is managed by a feedback controller operating on the variable speed pump P2. In particular, such controller receives temperature measurements from the bottom of TK (i.e., solar collector inlet temperature) and the outlet pipe of solar collector loop.

The controller returns a control signal varying P2 flow rate in order to achieve the desired outlet set point temperature (180°C). In addition, the controller also stops the pump P2 when simultaneously SC outlet temperature is lower than TK bottom temperature and the incident radiation falls below 100 W/m^2. In this case heat dissipations through the solar field are avoided. The heat exchanger HE is normally bypassed, but if the outlet temperature from solar collectors is greater than a set point value (250°C), the fluid enters HE to be cooled down to temperatures lower than 250°C. This is obtained by modulating the flow of on the secondary side of HE. Obviously the heated water is used as DHW. Therefore, the TK heat side is supplied by the hot diathermic oil obtained by the solar thermal collectors. Fixed speed pump P1 pumps the hot diathermic oil on the load side of the tank to the ORC. Which works at fixed inlet flow rate and temperature.

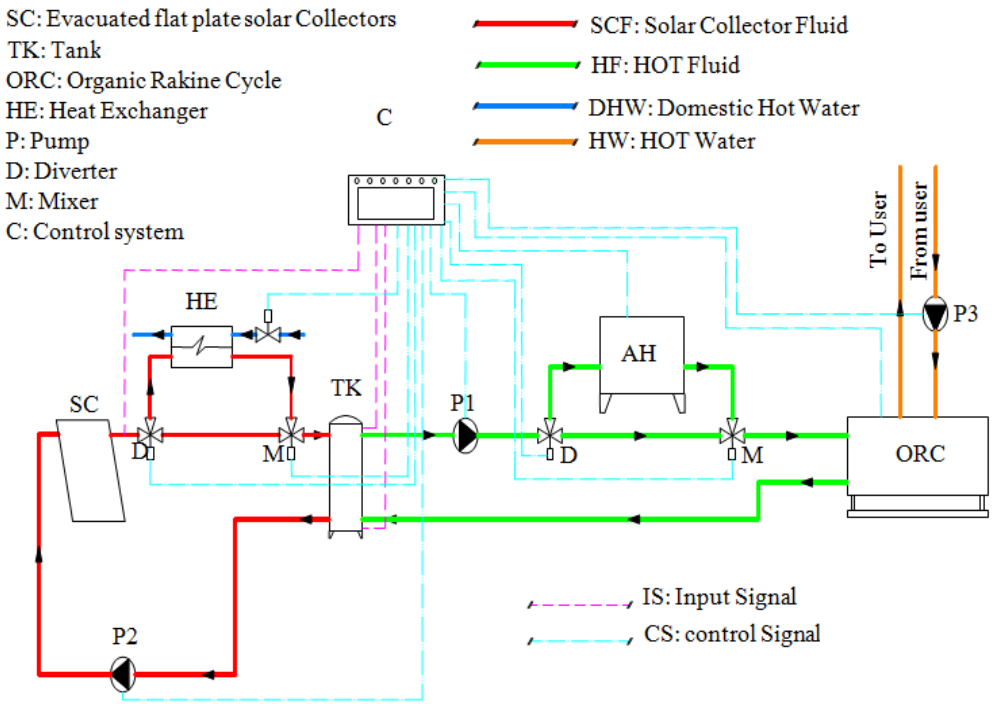

Fig. 1. System layout

If the P1 outlet oil temperature is lower than the desired set point temperature (180°C), the fluid passes through the gas fired boiler. Here the supplementary thermal energy is provided in order to reach the above mentioned set-point temperature.

Then, by ORC system electricity is produced and in addition by the cooling water at ORC condenser, hot water at low-medium temperature is also obtained for space heating purposes (by using fan-coils and radiant floors). ORC operation is discontinuous.

In fact, for avoiding high consumption of the auxiliary burner, if TK top temperature is lower than 152°C, pump P1 and consequently ORC system are stopped.

Afterwards, when the TK top temperature increases again and is greater than 180°C, by the produced thermal energy of solar collectors, pump P1 and ORC system are activated again. They remain activated until the top temperature of TK is higher than 152°C. This difference of temperature is high (180 and 152°C) in order to avoid the continuous deactivation and activation of ORC system. Thus such system produces simultaneously electricity and heat. Solar radiation and gas are the used fuels. By the suitable installed area of the solar collectors and definition of set-point temperatures, the appropriate use of both fuels is determined.

System Model

The plant above showed was simulated in TRNSYS environment, a software usually used for evaluating the dynamic performances of several systems/plants. The program consists of a library of built-in components, often validated from experimental point of view (Klein, 2006). This approach was also adopted by some of the authors in other studies (e.g., (Calise, 2010)), where also user-developed models are used and described.

In this section, only the description of the most important devices models, called "types" in TRNSYS, is provided. In particular the described components are: Storage Tank (TK), Organic Rankine Cycle (ORC) and Flat-plate evacuated Solar Collectors (SC).

The models of the others components (controllers, gas-fired burner, heat exchangers, pumps, etc.) are widely discussed in reference (Calise, 2010). Note also that all the components models are validated by experimental data.

In particular, the flat-plate evacuated solar collector model is validated by indoor-outdoor tests performed according to EN 12975 and EN 12976 ((ITW, 2012).

In addition this model was adopted by TVP solar in various projects. Such model was also successfully used by the authors in recent studies (Buonomano *et al*., 2014a; 2015; Calise *et al*., 2015). The model of the ORC is based on a data lookup approach based on manufacturer's data (Calise *et al*., 2012b).

Therefore, this model can be considered intrinsically validated since it reports real system operating data.

The models of all the other components (pumps, heat exchangers, tanks, etc.) were taken from TRNSYS library and/or from authors' previous works and they were all validated Vs. experiments (Buonomano *et al*., 2013; 2013b; 2014b; 2012; Calise *et al*., 2013b; Klein, 2006).

Nevertheless, because in literature the experimental validation of such plant is not still carried out, the whole system is not validated. However, the obtained results of the all carried out simulations can be evaluated very consistent as all components models (TRNSYS built-in and user-developed models) are experimental validated.

Solar Collectors

The innovative solar thermal collector devise included in this study has been recently presented by TVP Solar (Calise *et al*., 2013b). Such company designs, develops and manufactures a series of high-performance flat-plate solar thermal collectors based on a proprietary technology for cooling and heating applications.

Special patented technologies are used in order to achieve ultra-high vacuum (from 10^{-4} to 10^{-9} mbar, depending on the operating temperature) in all the operating conditions such as:

- an innovative flexible glass-metal sealing made from inorganic material (Fig. 2) which prevent any hydrogen atoms to entry from the surrounding area
- a getter adopted to maintain the high vacuum throughout the service life of the collector by absorbing hydrogen atoms (Calise *et al*., 2015)

On the basis of these technologies a complete series of evacuated collectors have been developed, optimized for low, medium and high temperature (respectively named LT-Power, MT-Power and HT-Power) applications up to 300°C.

In particular, during the past few years, TVP Solar performed a significant effort to develop MT-Power collectors. Such collectors are optimized to operate within the range 100°C-200°C and they are currently available for purchase and Solar Keymark certified by ITW Stuttgart (see certificate report 11COL1028).

Simultaneously, on the basis of the research and development work performed for MT-Power collectors, the company also developed HT-Power collectors, optimized for a high temperature range of applications (200-250°C).

Such the HT-Power collectors (version 4.0) are adopted in the present work. They include 2 exit ports and an inside serpentine (Fig. 3).

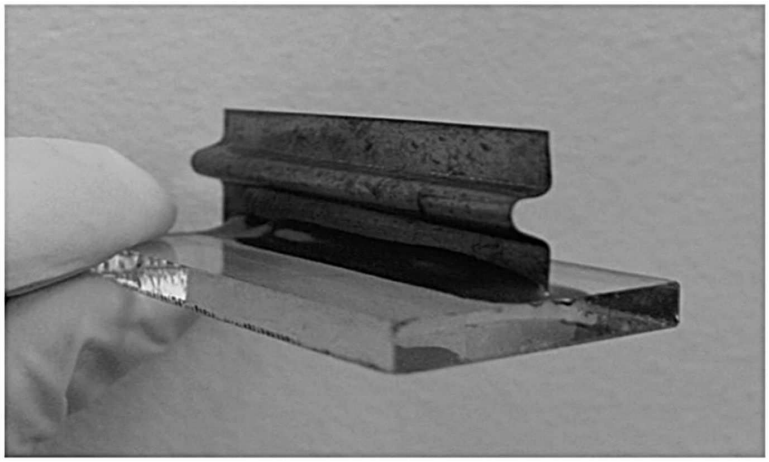

Fig. 2. Glass-Metal sealing (Calise *et al*., 2015)

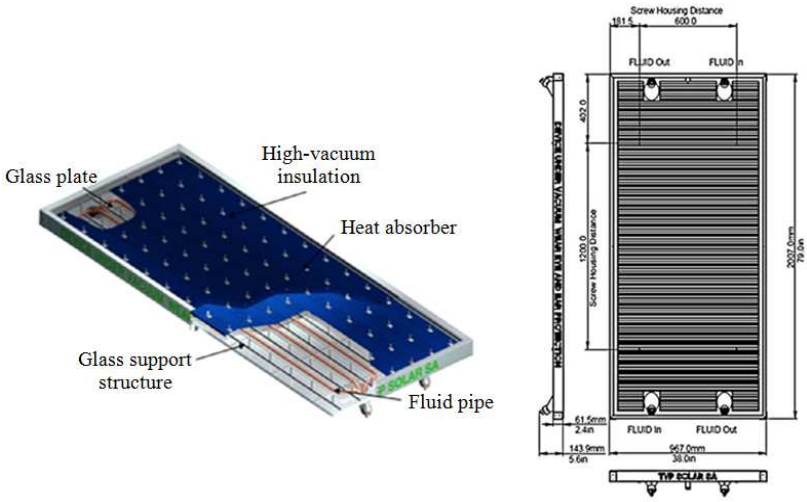

Fig. 3. Flat-plate deep evacuated solar collector (Calise *et al*., 2015)

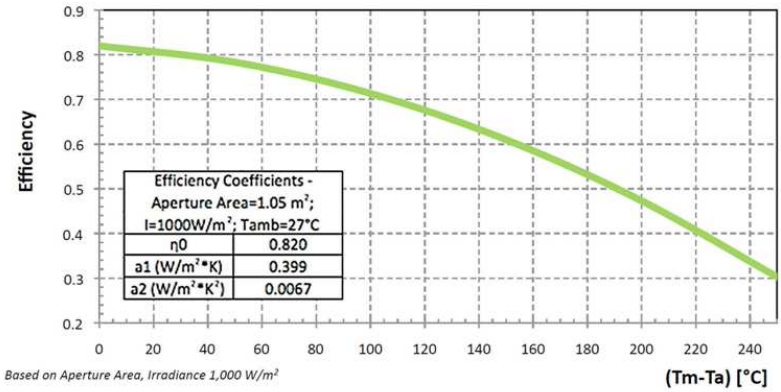

Incidence Angle Modifier (IAM) Coefficients								
Einfallswinkel θ *incident angle θ*	0	20	30	40	50	60	70	90
$K_{ec}(\theta)$:	1	0.99	0.98	0.95	0.91	0.84	0.70	0.00

Fig. 4. Efficiency curve of HT-Power panels v. 4.0

The high-vacuum allows HT-Power collectors to achieve very high efficiencies up to 200°C, as shown Fig. 4. Such graph shows that for T_m-T_a equal to 180°C (assuming 200 and 20°C, collector average temperature, T_m and ambient temperature, T_a, respectively) the efficiency is higher than 50%.

Conversely, when collector operating temperature rises to 250°C (T_m-T_a equal to 230°C), the efficiency decreases to about 35%. Note that collector stagnation temperature is 340°C.

This collector typically used pressurized water (20 bar) as operating fluid which can be used up to 200°C in order to avoid evaporation within the collector.

Therefore, in case of pressurized water, the adopted fluid (maximum operating temperature is 200°C) limits the maximum temperature of operating and not by the characteristics of the collector (stagnation temperature is 340°C).

Conversely, in case of highly-efficient diathermic oils (operating up to 370°C) or other potential fluids (steam, molten salts, etc.), the maximum collector operating temperature is limited by its stagnation temperature (e.g., by collector characteristics) and not by fluid thermodynamic constraints.

However, for long-time operation, to reduce possible mechanical and thermal stresses, temperatures below 250°C are suggested.

Based on Solarkeymark data, the high efficiencies reported in Fig. 4 are intensely greater than the evacuated-tube collectors efficiencies and also greater than the efficiencies of compact parabolic concentrating collectors (Calise *et al*., 2015).

This is due to several simultaneous effects:

- TVP collectors can convert both beam and diffuse radiation
- TVP heat losses are extremely low due to the ultra-high vacuum of such devices
- excellent radiative properties of the glass and coating

Thanks to the ultra-high vacuum insulation, this collector is scarcely sensitive to convective losses. Conversely, as all the other solar thermal collectors, such collector suffers for optical and radiative losses. However, optical losses are limited by an ultra-transparent glass (equipped with two anti-reflective coatings, one on each side).

Similarly, a special effort has been also performed to reduce radiative losses which may significantly affect collector efficiency during the high-temperature operation.

To this scope a special optimized selective coating is adopted, due to its lower dependence of emissivity as function of absorber temperature.

It is also worth noting that such high operating temperatures are achieved without solar concentration, avoiding tracking mechanisms and the need of special reflectors cleaning, resulting in much reduced system capital and operating costs (Calise *et al*., 2015).

The main data of the collector are summarized in Table 1.

As above reported, the latest version of HT-Power panels (v. 4.0), soon commercially available, is used for the solar field.

In the arrangement of such panels, the conventional string and arrays pipes and the solar collectors outlet flow rate are all at high level vacuum insulation (Fig. 5) (Palmieri *et al*., 2009).

In this case a reduction of the insulated external material piping by making available the return amount of the circulation path by the collectors themselves. In addition the heat losses reduce due to the properties of top insulation of high-vacuum in comparison to usual insulating materials (Calise *et al*., 2015).

In fact, as mentioned before, vacuum insulation dramatically reduces convective losses, whereas radiative losses are limited by the selective coating of the absorber as above discussed.

The adopted solar system configuration, reported in Fig. 5 (left), includes: A return main pipe and a supply main pipe, respectively arriving at the outlet high temperature and departing from the inlet low temperature; several branches each composed by a series of panels. By well-disposed parts (equipped by a custom shell semi-rigid insulating enclosure) the panels are interconnected. This allows to obtain a reduction of installation time and high performances.

Table 1. HT-Power specifications (Calise *et al*., 2015)

Parameter	Value	Unit
Length	967	mm
Height	2007	mm
Gross Area	1.95	m^2
Aperture Area	1.84	m^2
Volume of fluid	1.2	L
Heat Absorber pipe	Copper	/
Absorber coating	Alanod Sunselect	/
Back-plate coating	Anti corrosion	/
Glass coating	Double sided anti reflective	/
Stagnation Temperature	340	°C
Max. operating pressure	40	bar
Pressure drop (100 L/h)	0.7	kPa

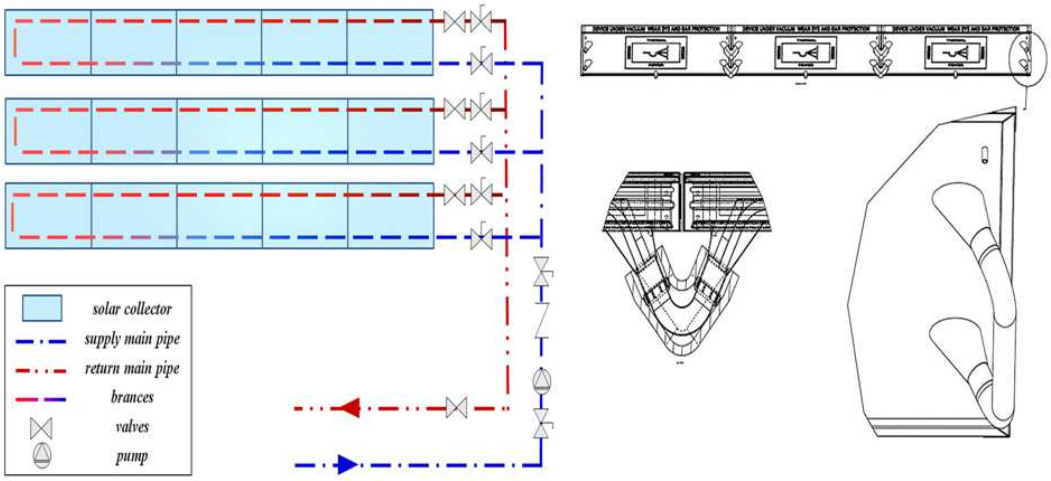

Fig. 5. Schematic of the solar field layout (left) and details of the interconnecting parts (right)

For calculating the thermal power transferred from the solar field to the SCF, the TVP HT-Power collectors are modelled by using the TRNSYS Type 132 (Bengt and Bales, 2002). This type is based on the Hottel-Whillier equation, with the adoption of the Incidence Angle Modifier coefficient (IAM).

This model can be used for both MT-Power and HT-Power collectors.

The simulation model was also validated by several experimental campaigns (both MT-Power and HT-Power) performed in different operating conditions. In this regard, many experimental data for different system layouts were obtained through outdoors and indoors solar tests (Buonomano *et al*., 2013a; 2013b; 2014b; Calise *et al*., 2013b; Klein, 2006).

The equation coefficients of HT-Power collector (see Fig. 4) were determined by simulations and indoor-outdoor tests, carried out according to EN 12975 and EN 12976 (ITW, 2012).

The HT-Power collector described in the study is a special enhancement of the MT-Power v3.11, which comes with a Solar Keymark certification by ITW Stuttgart (see certificate report 11COL1028).

Conversely, a Solar Keymark certification is not presently available for HT-Power collectors. Therefore, the performance coefficients for the novel HT collector (used in this study) have been obtained by experimental tests performed by the manufacturer. Although a certification for HT collector is still pending, such performance coefficients are well compatible with those of the Solar Keymark certified collector (MT-Power) when considering key differences in material parameters (see certificate report 11COL1028).

The better performance of the HT-Power collector compared with the MT-Power one is due to: (i) A selective coating (optimized for high-temperature operation); (ii) a more transparent glass; (iii) a larger size, reducing conduction losses. The key parameters for MT-Power Solar Keymark certified and HT-Power are presented in Table 2.

The main model equations are reported in the following. In particular, the solar collector output power per unit aperture area is calculated as:

$$P_{out} = F'\cdot(\tau\alpha)_{en}\cdot K_{\theta}(\theta)\cdot I - a_1\cdot(t_m - t_a) - a_2\cdot(t_m - t_a)^2$$
$$-a_3\cdot u\cdot(t_m - t_a) + a_4\cdot(E_L - \sigma T_a^{\,4}) - a_5\cdot\frac{dt_m}{dt} - a_6\cdot u\cdot I$$

where, I is the total solar radiation, sum of the beam, I_b and diffuse, I_d, solar radiation; $F'\cdot(\tau\alpha)_{en}$ is the zero loss efficiency of the collector at normal incidence angle for the solar radiation onto the collector; $K_{\theta}(\theta)$ is the IAM dependence of the zero loss efficiency.

In Equation 1, the wind dependence is modelled by taking into account the wind effect on the zero loss efficiency ($a_6\cdot u\cdot I$) and the wind influence on the heat losses ($a_3\cdot u\cdot(t_m - t_a)$), while the heat loss due to the long-wave radiation exchange is assumed equal to $a_4\cdot(E_L - \sigma T_a^{\,4})$.

In addition, at the second member of Equation 1, the first term can be calculated as:

$$F'\cdot(\tau\alpha)_{en}\cdot K_{\theta}(\theta)\cdot I = F'\cdot(\tau\alpha)_{en}\cdot\left[1 - b_0\cdot\left(\frac{1}{\cos\theta_b} - 1\right)\right]\cdot I_b +$$
$$F'\cdot(\tau\alpha)_{en}\cdot K_{\theta d}\cdot I_d$$

where, $\left[1 - b_0\cdot(1/\cos\theta_b - 1)\right]$ is the IAM for the beam radiation (b_0 is determined by collector tests); θ_b is the incidence angle for beam radiation; $K_{\theta d}$ is the IAM for the diffuse radiation.

Table 2. Main differences between MT-Power (certified) and HT-Power properties

Panels	MT-Power (certified)	HT-Power
Selective Coating Absorptivity	0.9200	0.9100
Selective Coating Emissivity (100°C)	0.0430	0.0350
Selective Coating Emissivity (200°C)	0.0590	0.0500
Selective Coating Emissivity (300°C)	0.0900	0.0720
Glass Transparency	0.9000	0.9500
Glass Emissivity (RT)	0.8400	0.8400
Bottom Emissivity (RT)	0.3000	0.3000
η_0	0.7590	0.8200
a_1	0.5080	0.3990
a_2	0.0070	0.0067

Storage Tank

Fundamental elements of solar systems are the heat storage devices which are used to smooth the discrepancy between energy supply and the heating and cooling demands. At the same time, systems performances highly depend on the simultaneity between solar resource availability and demand. A mismatch between the supply and the demand often occurs during the system operation. Thus, in order to balance the energy requirements and to limit such mismatch, it is necessary to exploit as much as possible the solar source. In order to achieve such goal, a stratified thermal storage tank was included. For modelling the tank the TRNSYS built-in Type 4d was used (Klein, 2006). The model is based on the assumption that the tanks can be divided into N fully-mixed equal sub-volumes. The tank is also equipped with a pressure relief valve, in order to account the boiling effects. The model takes into account the energy released by the fluid flowing through the valve, whereas the corresponding loss of mass is neglected. The temperatures of the N nodes are calculated on the basis of unsteady energy and mass balances. The energy balance on the i-th tank layer can be written as follows:

$$M_i c_{p,f} \frac{dT_i}{d\vartheta} = \alpha_i \dot{m}_H c_{p,f} \left(T_H - T_i\right) + \beta_i \dot{m}_L c_{p,f} \left(T_L - T_i\right) + UA_i \left(T_a - T_i\right) + \gamma_i c_p \left(t_{i-1} - t_i\right)$$

The control function γ_i is defined as follows:

$$\gamma_i = \dot{m}_H \sum_{j=1}^{i-1} \alpha_j - \dot{m}_L \sum_{j=i+1}^{N} \beta_j$$

The coefficient α_i and β_i are equal to 1 if the i-th segment corresponds to the top and to the bottom of the tank, respectively; otherwise they are set to 0.

Organic Rankine Cycle

A complete model of an ORC cycle is out of the scope of this work. In fact, according to the control strategy before discussed, the ORC used in this system operates at constant oil inlet temperature and flow rate.

As a consequence, the model does not need an accurate-but time-consuming-simulation of the whole ORC system in order to account for its part-load operation. As a consequence, in this study the ORC is simulated by using a data lookup approach, as usually occurs in dynamic simulations for several components such as absorption chillers, reciprocating engines, etc. (Calise, 2012; Calise *et al*., 2011a; 2012a; 2012b). In particular, this study is based on a commercially available 10 kW_e ORC system.

The ORC is designed for a nominal electrical capacity of 10 kW when supplied by 6000 kg/h at 180°C. The ORC operates according to a simple Rankine cycle without regenerative heat exchanger. It uses R245fa as working fluid.

The rated electrical efficiency is 10%. The manufacturer provides a comprehensive lookup table including the performance data of the ORC in all the operating conditions. In particular, the lookup table provided by the manufacturer includes values of thermal heat and electrical powers for all the operating conditions (Calise *et al*., 2012b).

Thermo-Economic Model

The energy analysis was performed by evaluating the eventual savings in terms of primary energy achieved by the solar power system, Vs. a conventional system assumed as a reference. In such Reference System (RS), a gas-fired boiler provides thermal energy, whereas electrical energy is provided by the grid. In RS η_b, gas-fired boiler thermal efficiency, is supposed equal to 80%, whilst $\eta_{el,t}$, thermoelectric power plant efficiency, is 46.1%.

By taking into consideration each time-steps of the operation time, the realizable primary energy saving by the proposed plant is:

$$\Delta PE = \sum_i \left(\frac{Q_{heat,ORC,i}}{\eta_b} - \frac{Q_{AH,i}}{\eta_{b,AH,i}} \right) + \frac{1}{\eta_{el,t}} \sum_i \left(E_{el,ORC,i} - E_{el,aux,i} \right)$$

Where:

$Q_{heat,ORC,i}$ = The thermal energy produced by the ORC (and/or by HE) and delivered to the user

$Q_{AH,i}$ = The gas-fired auxiliary heater thermal energy
$E_{el,ORC,i}$ = The electricity produced by the ORC
$E_{el,aux,i}$ = The auxiliary electricity for the devices as well as the pumps used in the proposed solar power plant

The Solar Fraction (F_{sol}) is also taken into consideration in order to evaluate the energy efficiency of such solar system. This parameter is calculated as the ratio between the thermal energy produced by the solar field (Q_{SC}) and the total energy provided to the users: $Q_{AH} + Q_{SC} = Q_{in,ORC}$:

$$F_{sol} = \frac{Q_{SC}}{Q_{in,ORC}} = \frac{Q_{SC}}{Q_{SC} + Q_{AH}}$$

In addition a complete economic model was developed for calculating the operating costs and capital costs. In reference (Calise *et al*., 2011b) the components (boiler, pumps, tank, etc.) cost functions (J_i) are reported.

As before mentioned, the majority of the commercial production of TVP Solar is based on MT-Power collectors, being HT-Power solar collectors in a pre-commercial stage. Therefore, the present capital cost of HT-Power solar collectors is still high due to the limited production. However, on the basis of manufacturer experience on MT-Power collectors and by taking into account the different material costs, the manufacturer estimates that in case of forthcoming massive production of their collectors, the capital cost of the HT-Power collectors may be around 350 €/m^2.

In the following discussion, simulation results (e.g., figures) related to the cost include the costs of the collectors and their installation, excluding Balance of System components (valves, pipes, fittings, etc.).

According to manufacturer's data Balance of System cost is expected equal to 30% of the collectors' capital cost. Similarly, according to manufacturer's data, capital cost of ORC system is assumed equal to 4500 €/kW$_e$.

The operating cost, C_{op}, takes into consideration:

- The AH natural gas consumption
- The maintenance, assumed equal to 1%/year of the capital cost of whole plant

In addition, the cash flow must also consider the savings due to production of thermal energy and electricity. In particular, unit costs of natural gas and electricity c_{NG} and c_{EE} are assumed respectively equal to 0.60 €/Sm^3 and 0.35 €/kWh. The latter takes into account the feed-in tariff presently used in Italy for solar power systems.

Thus, the yearly saving obtained by the solar power systems is defined as:

$$\Delta C_{op} = \sum_i \left(\frac{Q_{heat,ORC,i} c_{NG,user}}{\eta_b} - \frac{Q_{AH,i} c_{NG}}{\eta_{b,AH,i}} \right) \frac{1}{LHV_{NG}} + c_{EE} \sum_i \left(E_{el,ORC,i} - E_{el,aux,i} \right) - 0.001 \sum_i J_i$$

Finally, the economic performance of the SHC system can be calculated by using the Simple Pay Back period (SPB), with and without incentives, as defined in reference (Calise *et al*., 2011a):

$$SPB = \left(\sum_i J_i \right) / \Delta C_{op}$$

In particular, four possible incentive strategies are considered in this study:

- Case SPB0: A feed-in tariff equal to 0.35 €/kWh is taken into consideration for the net electricity production
- Case SPB1: No feed-in tariff
- Case SPB2: A feed-in tariff equal to 0.35 €/kWh is taken into consideration for the net electricity production and public funding equal to 40% of the capital cost
- Case SPB3: A feed-in tariff equal to 0.35 €/kWh is taken into consideration for the net electricity production and a feed-in tariff equal to 0.20 €/kWh for the net thermal energy production

Results and Discussion

By the simulation model above discussed, a case study was developed for a building located in Naples, South of Italy.

The prototype will be installed on the roof of the building. The overall electrical and thermal production of the system will be consumed by the householder. Thermal energy will be used for space heating and domestic hot water.

The system is dynamically simulated in TRNSYS environment, obtaining results on any time basis (years, months, weeks, etc.). This methodology allows one to design the system by appropriately selecting all the synthesis/design parameters. In addition, such approach also returns detailed charts of temperatures and energy flows to be used as guidelines in order to select the appropriate operation strategies for the system under investigation.

The case study was developed by using the design and operational parameters summarized in Table 3. Here, the system is designed starting from the electrical capacity of the ORC, which is 10 kW. Under nominal conditions (oil inlet temperature of 180°C and flow rate of 6000 kg/h) ORC efficiency is 10%. Therefore, the thermal input of the ORC should be 100 kW. As a consequence, both solar field and boiler were selected in order to match this peak demand.

Table 3. System main design parameters

Parameter	Description	Value	Unit
N_{SC}	Number of Solar Collectors	110.0000	/
$A_{SC,u}$	Solar Collector Aperture Area	1.8400	m^2
q_{P2}	P2 flow rate per unit SC aperture area	45.0000	kg/hm^2
v_{TK}	Tank TK Volume per unit SC aperture area	10.0000	l/m^2
η_0	SC Zero loss efficiency at normal incidence	0.8200	-
a_1	1^{St} order SC heat loss coefficient	0.3990	W/m^2K
a_2	2^{nd} order SC heat loss coefficient	0.0067	W/m^2K
c_f	Diathermic oil specific heat	2.1200	kJ/kg K
α	Collector Slope	30.0000	°
α	Collector Azimuth	0.0000	°
$T_{set,SC}$	SC outlet set point temperature	180.0000	°C
$T_{set,AH}$	AH outlet set point temperature	180.0000	°C
$T_{TK,min}$	Minumum value of TK top temperature for ORC activation	152.0000	°C
$T_{TK,act}$	Value of TK top temperature for ORC re-activation	180.0000	°C
q_{P1}	P1 flow rate	6000.0000	kg/h
$Q_{AH,rated}$	Rated AH heat capacity	120.0000	kW
$P_{ORC,rated}$	Rated AH electrical capacity	10.0000	kW
$\eta_{ORC,rated}$	Rated AH electrical efficiency	10.0000	%

Table 4. Yearly results: Energy (MWh/y)

Parameter	Value
I_{tot}	351
Q_{SC}	122
Q_{AH}	41
PE_{AH}	48
$E_{el,ORC}$	16
$E_{el,aux}$	2
$Q_{cog,ORC}$	143
ΔPE	161

Table 5. Yearly results: Economics

Parameter	ΔC_{op}	J_0	SPB	NPV	PI
Unit	k€/y	k€	y	k€	-
Value	17	137	8	74	1

Table 6. Yearly results: Main efficiencies

Parameter	F_{sol}	η_{SC}	η_{AH}	η_{ORC}
Value	74.8%	34.8%	85.6%	10.1%

This resulted in a solar field area of 202 m^2 and an auxiliary heater capacity of 120 kW. The collector field is installed facing south and an inclination respect to the horizontal equal to 30° is assumed.

The yearly simulation (8760 h) is performed by using the weather data of Naples, included in the Meteonorm database. A small time-step of 0.04 h is used in order to promote the convergence in capacitive components, such as the storage tank TK.

The yearly results of the simulation are shown in Table 4 to 6.

The most important yearly energy flows are summarized Table 4.

The overall radiation incident, I_{tot}, on the solar field is 351 MWh/y. Such value corresponds to a radiative flow of 1.73 kWh/m^2 (usual for Southern Mediterranean zones).

The overall thermal production by the solar collector, Q_{SC}, is 122 MWh/y, whilst much lower (41 MWh/y) is the thermal energy of gas-fired auxiliary burner, Q_{AH}.

The overall electrical production, $E_{el,ORC}$, of the ORC is 122 MWh/y, not particularly high for a 10 kW system. In fact, it corresponds to 1600 h of full operation per year.

This result derives from the control strategy adopted in this study. In fact, the ORC system is switch off if the TK top temperature is lower than $T_{TK,min}$ (152°C) and it is again activated only if such temperature became again equal to $T_{TK,act}$ (180°C).

Therefore, during the daytime the ORC is often not operating for several hours. Such control avoids a high gas-fired burner consumption. It is worth noticing that the electricity provided to electrical auxiliary components (pumps) is considerably lower than the ORC electricity production. Also the cogenerative heat produced by the ORC, $Q_{cog,ORC}$, is also high (143 MWh/y), even higher than the total production of thermal energy by the solar collectors. Obviously, such cogenerative heat of the ORC is only available at low temperature (45°C), contrary to the fluid exiting from the solar field. The overall yearly savings in terms of primary energy, ΔPE, is 161 MWh/y.

The economic results of the simulation are shown in Table 5.

The total cost of the system, J_0, is 137 k€ and it is mainly due to the ORC (33%) and to the solar collectors (52%). The global specific cost of the plant is considerably higher (13.7 € per W of electrical power), compared to present day photovoltaic system, however, the system under investigation produces not only electricity but also large amounts of thermal energy and

can benefit of hefty incentives. This results in yearly savings, in terms of operating costs, ΔC_{op}, equal to 17 k€/y and consequently the Simple Pay Back (SPB) period is about 8 years. The Net Present Value (NPV) for the system is 74 k€ and the Profit Index ($PI = NPV/J_0$) is also good at 0.54. In summary, the economic analysis of the considered configuration shows good profitability. These results are basically due to the excellent efficiency (η_{SC}) of the solar collector field, as shown in Table 6. In fact, an average efficiency of 34.8% operating around 180°C is an unprecedented result.

With the present configuration, the majority of the heat required to drive the ORC is produced by the solar field, being the solar fraction (F_{sol}) about 74.8%. The average efficiency of the ORC (η_{ORC}) is very close to the nominal one, with a very stable operation due to the almost constant inlet oil temperature and flow rate.

As expected, the solar power system under investigation is particularly sensitive to the weather conditions, especially the solar radiation. The weekly integrated produced energies, shown in Fig. 6, dramatically decrease during the winter. In particular, Fig. 6 shows that in winter I_{tot}, the total incident solar radiation, is particularly low with respect to the one available in summer. This circumstance determines a remarkable decrease of thermal energy produced by the solar field, Q_{SC}, during the coldest winter weeks. As a consequence, in such weeks the tank temperature is in general low and the activation time of the ORC rather brief.

This results in a reduced amount of heat used by the ORC, $Q_{in,ORC}$, in winter (Fig. 7) and a consequent lower overall electrical production, $E_{el,ORC}$. However, Fig. 7 also shows that the thermal energy required to the auxiliary burner does not increase during winter. In fact, the control strategy proposed in this study prevents a high and unwanted consumption of the burner, deactivating AH and ORC if TK top temperature is lower than 152°C. Figure 7 also shows a slight difference between the inlet TK thermal energy (from solar field), $Q_{TK,in}$ and the one delivered to the ORC, $Q_{TK, out}$. In a weekly analysis such difference is due only to the losses to the environment. However, considering a smaller time-base the difference may be more significant as a consequence of the capacitive behaviour of the tank.

This is even clearer in Fig. 8 where η_{TK}, the inlet TK thermal energy with respect to outlet TK thermal energy, is shown. This efficiency is particularly low in the first week. This is due since the high amount of inlet TK thermal energy is required for increasing the TK inside oil temperature from 20°C (initial temperature value) up to 180°C. As a consequence, the amount of heat delivered to the ORC is much smaller than the one received from the solar field. Then, η_{TK} is almost constant and its value is essentially due to the heat losses towards the outdoor environment.

Figure 8 also shows that both η_{ORC} and η_{AH} (ORC and AH efficiencies, respectively) do not considerably vary during the time. In fact, ORC boundary conditions are almost constant and in addition the variations of inlet fluid temperature and/or environmental temperature do not influence the efficiency of auxiliary burner.

Conversely, the efficiency of the solar collectors fluctuates during the year, being close to 40% in summer and down to 20% in winter (in the coldest weeks). Solar fraction is constant at about 75% as a result of the control strategy above discussed.

Figure 9 shows the capability of the tool developed in this study to simulate the real behaviour of the system.

Here, for a typical day of summer operation the thermal and electrical power are depicted. It is shown that ORC is deactivated until 10:00 am since the temperature in the tank is below 180°C. However, during the early morning the solar field is producing heat delivered to the storage thermal tank. Thus, the tank temperature increases up to 180°C until about 10:00 am when the ORC and AH are re-activated.

During the central hours of the day, the ORC operates at full load, i.e., the solar field drives its thermal demand. Only in the late evening same auxiliary heat must be supplied by the gas-fired burner, in order to achieve a constant inlet temperature for the ORC.

As before mentioned, the overall performance of the system is very sensitive to even small variations of its design and operational parameters. Therefore, a parametric analysis aiming at evaluating the variations of system energetic and economic performances as a function of such parameters has been performed. As expected, the total solar field area plays a crucial role in the thermo-economic performance of the system. In fact, Fig. 10 shows that all thermal energy flows increase when the SC area is higher. In particular, thermal energy produced by SC linearly increases with its capacity. This corresponds a slight increasing of the thermal and electricity production of ORC system. In fact, the higher the capacity of the solar field, the higher the average temperature of the tank TK, which in turn increases the number of operating hours of the ORC. It is worth noting that the increase of SC thermal production is much higher than the corresponding increase of ORC thermal demand and electrical production. This is due to the fact that in the considered parametric analysis the capacity of the ORC is kept constant (since only one parameter per time is varied). Therefore, this circumstance limits a possible further enhancement of ORC electrical production.

Conversely, the heat supplied by the gas-burner decreases with increasing the temperature of the HTF exiting from the tank. For large solar fields (higher than 400 m^2) the heat exchanger HE starts to produce an additional amount of heat for domestic hot water.

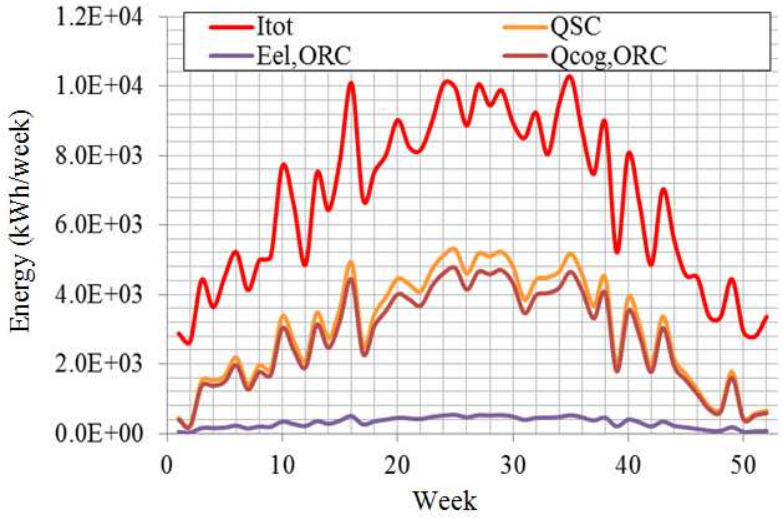

Fig. 6. Weekly electrical and thermal energy (1)

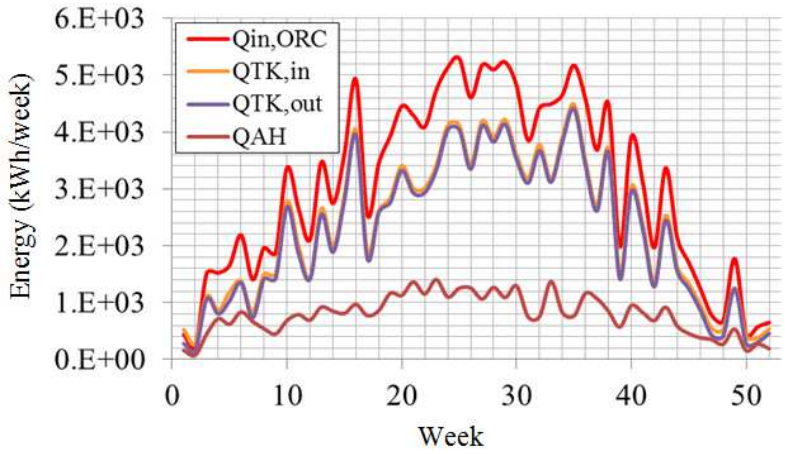

Fig. 7. Weekly thermal energy (2)

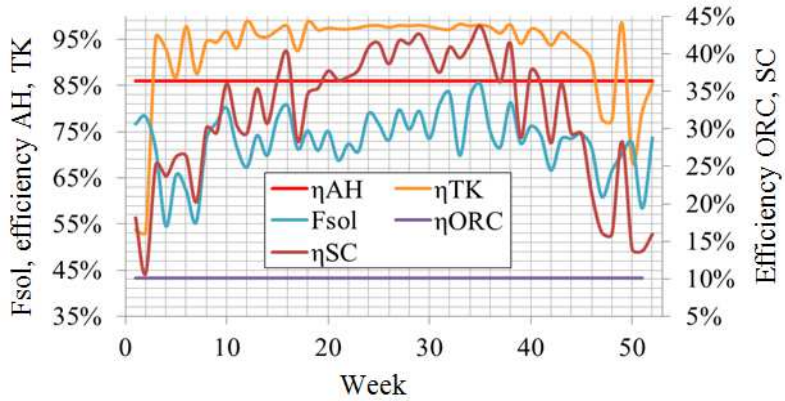

Fig. 8. Weekly solar fraction and efficiencies

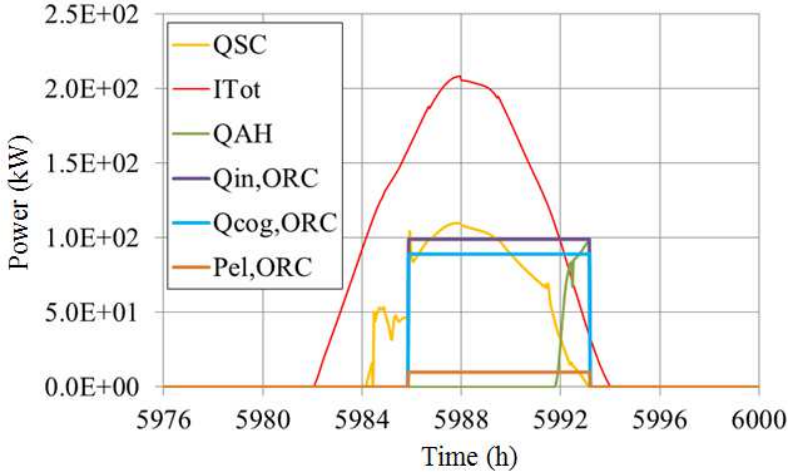

Fig. 9. Summer day: Thermal and electrical powers

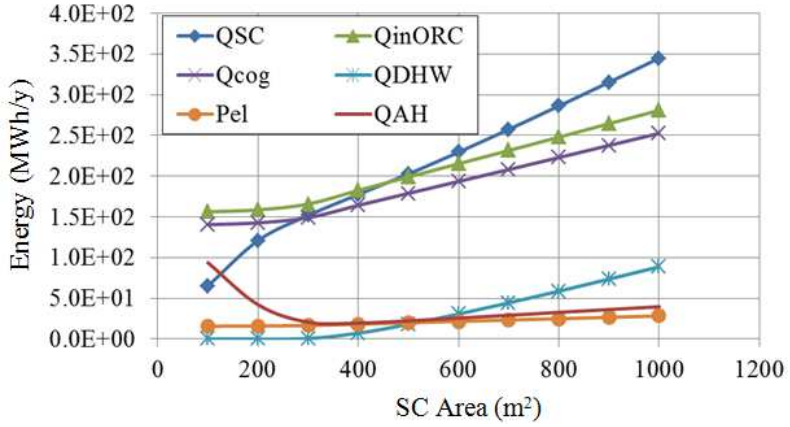

Fig. 10. Sensitivity analysis: Thermal and electrical energy Vs collector area

This means that, for large solar fields, SC outlet temperature may be often higher than 250°C. In fact, SC outlet temperature depends on a number of parameters, such as: Flow rate, inlet temperature, solar radiation, etc. In the carried out parametric analysis, all the above mentioned parameters are almost constant, except for the average SC inlet temperature. For large solar fields, tank temperature-and consequently SC inlet temperature-rises because the increase of ORC heat demand (at fixed capacity) is lower than the corresponding increase of solar field heat production.

In fact, Fig. 10 shows that the slope of the SC thermal energy (Q_{SC}) is much higher than the one of the thermal energy demanded by the ORC system ($Q_{in,ORC}$). This circumstance is due to same assumed ORC capacity, which is not dependent on the solar field area.

Therefore, in case of large solar fields a mismatch is observed between solar production and ORC thermal demand. Obviously, this mismatch between production and demand determines an increase of tank temperature (thermal input higher than thermal output). This mismatch results in a higher production by HE, which is activated only when SC outlet set point temperature is higher than the fixed set point.

The economic analysis is shown in Fig. 11. Here, the best configuration for the majority of the funding scenarios is achieved when the SC area is around 200 m^2. When no incentive is provided for the thermal energy produced, the optimum configuration is obviously achieved for the lowest SC area.

An increase of the tank volume is not profitable from both energetic and economic points of view, as shown in Fig. 12 and 13. In fact, a high volume of the tank corresponds an increasing of its heat losses toward the environment. In addition, large storage volumes are not recommendable since they dramatically increase system inertia. In fact, in case of large volumes, the solar collectors require longer periods time in order to obtain the wanted set point temperature.

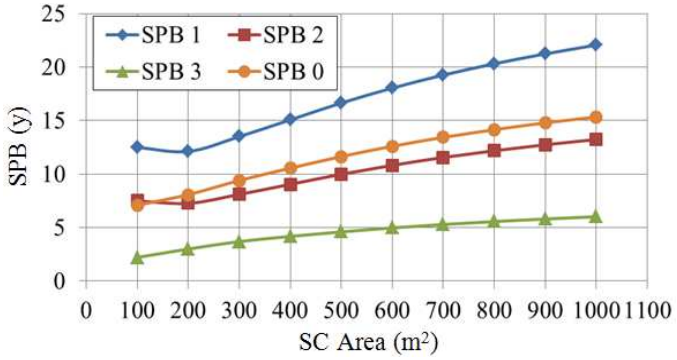

Fig. 11. Sensitivity analysis: Simple Pay Back Vs solar collector area

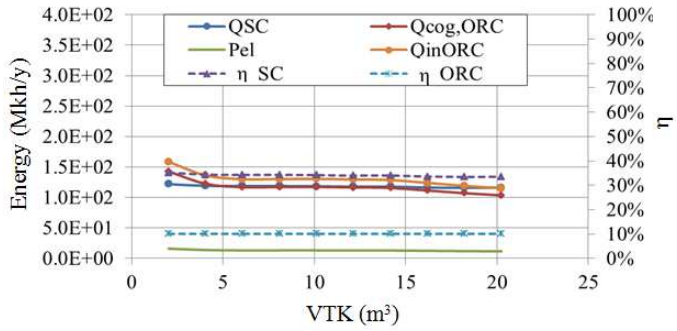

Fig. 12. Sensitivity analysis: Thermal and electrical energy Vs TK volume

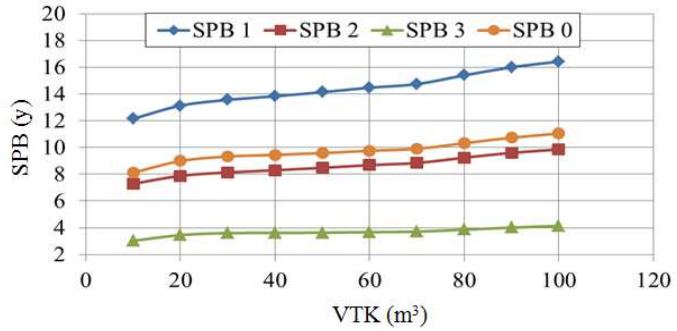

Fig. 13. Sensitivity analysis: Simple Pay Back Vs TK volume

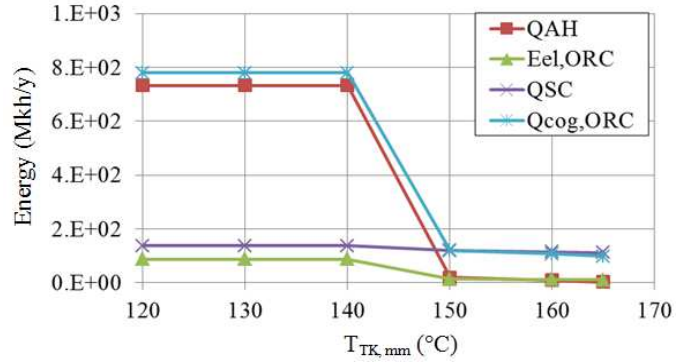

Fig. 14. Sensitivity analysis: electrical and thermal energy Vs $T_{TK,min}$

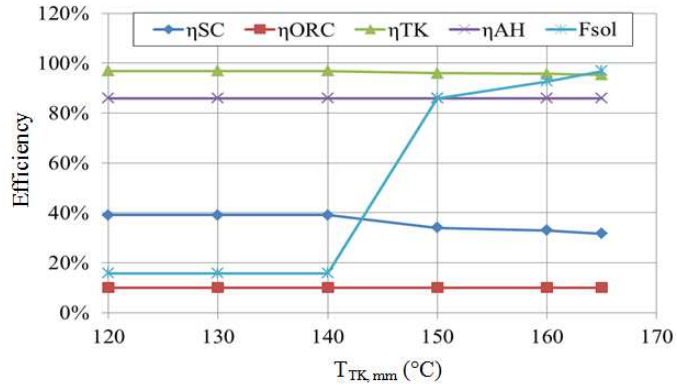

Fig. 15. Sensitivity analysis: Solar fraction and efficiencies Vs $T_{TK,min}$

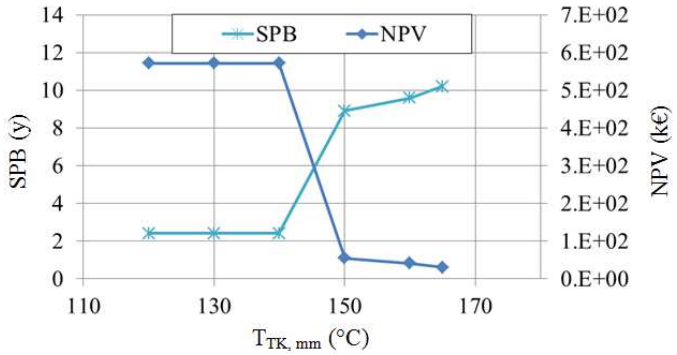

Fig. 16. Sensitivity analysis: Simple Pay Back and Net Present Value Vs $T_{TK,min}$

Therefore, in case of large storage volumes, temperature in TK is averagely lower than the one achievable with smaller tanks.

In summary, increasing storage volume does not determine any improvement in system electrical and thermal productions, but obviously determines high capital costs. The overall result, from the economic point of view, is a SPB increasing with storage volume, for any considered incentive scheme.

Finally, simulation results are also sensitive to the values of set-point temperatures fixed in the control strategy. In fact, Fig. 14 to 16 show the sensitivity analysis varying $T_{TK,min}$, i.e., the temperature for ORC re-activation, as discussed above. This parameter is crucial for determining the system solar fraction. In fact, when $T_{TK,min}$ is low, TK average temperature is also low. As a consequence a large amount of thermal energy must be supplied by the auxiliary heater in order to reach ORC inlet set-point temperature.

Therefore, the higher $T_{TK,min}$, the lower Q_{AH} and the higher the solar fraction. It also worth observing how the slope of the curve dramatically increases around 140°C. In fact, during the operation, TK top temperature rarely falls below that temperature. At nominal conditions, the temperature of diathermic oil exiting from ORC is 152°C.

The tank TK is a stratified tank in which the flow enters the tank at the node at the same temperature of the inlet flow. Therefore, even when the bottom part of TK is cold, the top one receives a stream at 152°C from ORC. This complex combination of temperatures determines the plots shown in Fig. 14 and 15.

From the economic point of view, Fig. 16 shows that the best configurations are achieved for low values of $T_{TK,min}$, where the solar fraction is also low.

Conclusion

The results of the presented case study highlight technical and economic feasibility of the analysed solar ORC power plant. The dynamic simulation shows that the system is capable to produce electricity and space heating all year long. The results of the dynamic simulations also show the significant potential of energy savings of the system under investigation, especially during the summer. In fact, thermal and electrical productions are much fluctuating, depending on external solar radiation and

temperature. Therefore, an auxiliary system is always mandatory for a safe operation of the system.

In conclusion, such solar power plant is principally affected by the solar radiation availability: During the cold winter days, when the average temperature of the fluid stored in the tank is significantly lower than ORC inlet set point. The study also shows that an suitable set point temperature is decisive for achieving a full utilization of the solar energy. Finally, a high volume of thermal storage tank are unprofitable from energy point of view and in particular from economic point of view. The economic profitability of such system is comparable with other similar solar heating, cooling and power systems investigated by the authors in the past few years (Buonomano *et al*., 2014a; 2013b; 2014b; 2013c; 2015; Calise, 2010; 2012; Calise *et al*., 2011a; 2012a; 2015; 2013b; 2011b; 2012b). Furthermore, the proposed solar power plant is particularly convenient with public funding policies. The system is extremely profitable when feed-in tariffs similar to those currently assumed in EU for solar power system are adopted. The economical profitability can be further enhanced when the feed-in tariff considers also the system thermal production (Al-Sulaiman and Fahad, 2014; Buonomano *et al*., 2013c; 2012; Calise *et al*., 2011b).

Funding Information

The authors have no support or funding to report.

Author's Contributions

All authors equally contributed in this work.

Ethics

This article is original and contains unpublished material. The corresponding author confirms that all of the other authors have read and approved the manuscript and no ethical issues involved.

References

Al-Sulaiman, A.F., 2014. Exergy analysis of parabolic trough solar collectors integrated with combined steam and organic Rankine cycles. Energy Convers. Manage., 77: 441-449. DOI: 10.1016/j.enconman.2013.10.013

Al-Sulaiman, F.A., F. Hamdullahpur and I. Dincer, 2012. Performance assessment of a novel system using parabolic trough solar collectors for combined cooling, heating and power production. Renewable Energy, 48: 161-172. DOI: 10.1016/j.renene.2012.04.034

Al-Sulaiman, F.A., I. Dincer and F. Hamdullahpur, 2011. Exergy modeling of a new solar driven trigeneration system. Solar Energy, 85: 2228-2243. DOI: 10.1016/j.solener.2011.06.009

Astolfi, M., L. Xodo, M.C. Romano and E. Macchi, 2011. Technical and economical analysis of a solar-geothermal hybrid plant based on an Organic Rankine Cycle. Geothermics, 40: 58-68. DOI: 10.1016/j.geothermics.2010.09.009

Bengt, P. and C. Bales, 2002. Report of IEA SHC-task 26, solar combisystems.

Bruno, J.C., J. López-Villada, E. Letelier, S. Romera and A. Coronas, 2008. Modelling and optimisation of solar organic rankine cycle engines for reverse osmosis desalination. Applied Thermal Eng., 28: 2212-2226. DOI: 10.1016/j.applthermaleng.2007.12.022

Bu, X.B., H.S. Li and L.B. Wang, 2013. Performance analysis and working fluids selection of solar powered organic Rankine-vapor compression ice maker. Solar Energy, 95: 271-278. DOI: 10.1016/j.solener.2013.06.024

Buonomano, A., F. Calise, M. Dentice d'Accadia and L. Vanoli, 2013a. A novel solar trigeneration system based on concentrating photovoltaic/thermal collectors. Part 1: Design and simulation model. Energy, 61: 59-71. DOI: 10.1016/j.energy.2013.02.009

Buonomano, A., F. Calise and G. Ferruzzi, 2013b. Thermoeconomic analysis of storage systems for solar heating and cooling systems: A comparison between variable-volume and fixed-volume tanks. Energy, 59: 600-616. DOI: 10.1016/j.energy.2013.06.063

Buonomano, A., F. Calise and A. Palombo, 2013c. Solar heating and cooling systems by CPVT and ET solar collectors: A novel transient simulation model. Applied Energy, 103: 588-606. DOI: 10.1016/j.apenergy.2012.10.023

Buonomano, A., F. Calise, M. D'Accadia Dentice, G. Ferruzzi and M. Scarpellino, 2014a. Design and simulation of a prototype of a small-scale solar power plant based on evacuated flat-plate solar collectors and Organic Rankine Cycle. Proceedings of the 27th International Conference on Efficiency, Cost, Optimization, Simulation and Environmental Impact of Energy Systems, (IES' 14).

Buonomano, A., F. Calise, G. Ferruzzi and L. Vanoli, 2014b. A novel renewable polygeneration system for hospital buildings: Design, simulation and thermo-economic optimization. Applied Thermal Eng., 67: 43-60. DOI: 10.1016/j.applthermaleng.2014.03.008

Buonomano, A., G. Mittelman, D. Faiman, S. Biryukov and V. Melnichak *et al*., 2012. Modelling an actively-cooled CPV system. AIP Conf. Proc., 1477: 235-238. DOI: 10.1063/1.4753876

Buonomano, A., F. Calise, A. Palombo and M. Vicidomini, 2015. Energy and economic analysis of geothermal-solar trigeneration systems: A case study for a hotel building in Ischia. Applied Energy, 138: 224-241. DOI: 10.1016/j.apenergy.2014.10.076

Calise, F., 2010. Thermoeconomic analysis and optimization of high efficiency solar heating and cooling systems for different Italian school buildings and climates. Energy Build., 42: 992-1003. DOI: 10.1016/j.enbuild.2010.01.011

Calise, F., 2012. High temperature solar heating and cooling systems for different Mediterranean climates: Dynamic simulation and economic assessment. Applied Thermal Eng., 32: 108-124. DOI: 10.1016/j.applthermaleng.2011.08.037

Calise, F., M.D. D'Accadia and L. Vanoli, 2011a. Thermoeconomic optimization of solar heating and cooling systems. Energy Convers. Manage., 52: 1562-1573. DOI: 10.1016/j.enconman.2010.10.025

Calise, F., G. Ferruzzi and L. Vanoli, 2011b. Transient simulation of polygeneration systems based on PEM fuel cells and solar heating and cooling technologies. Energy, 41: 18-30. DOI: 10.1016/j.energy.2011.05.027

Calise, F., M.D. D'Accadia and L. Vanoli, 2012a. Design and dynamic simulation of a novel solar trigeneration system based on hybrid Photovoltaic/Thermal collectors (PVT). Energy Convers. Manage., 60: 214-225. DOI: 10.1016/j.enconman.2012.01.025

Calise, F., A. Palombo and L. Vanoli, 2012b. Design and dynamic simulation of a novel polygeneration system fed by vegetable oil and by solar energy. Energy Convers. Manage., 60: 204-213. DOI: 10.1016/j.enconman.2012.02.014

Calise, F., C. Capuozzo and L. Vanoli, 2013a. Design and parametric optimization of an organic rankine cycle powered by solar energy. Am. J. Eng. Applied Sci., 6: 178-204. DOI: 10.3844/ajeassp.2013.178.204

Calise, F., M. Dentice d'Accadia, A. Palombo and L. Vanoli, 2013b. Dynamic simulation of a novel high-temperature solar trigeneration system based on concentrating photovoltaic/thermal collectors. Energy, 61: 72-86. DOI: 10.1016/j.energy.2012.10.008

Calise, F., M.D. D'Accadia, M. Vicidomini and M. Scarpellino, 2015. Design and simulation of a prototype of a small-scale solar CHP system based on evacuated flat-plate solar collectors and Organic Rankine Cycle. Energy Convers. Manage., 90: 347-363. DOI: 10.1016/j.enconman.2014.11.014

Dai, Y., J. Wang and L. Gao, 2009. Parametric optimization and comparative study of Organic Rankine Cycle (ORC) for low grade waste heat recovery. Energy Convers. Manage., 50: 576-582. DOI: 10.1016/j.enconman.2008.10.018

Delgado-Torres, A.M. and L. García-Rodríguez, 2010a. Analysis and optimization of the low-temperature solar ORGANIC RANKINE CYCLE (ORC). Energy Convers. Manage., 51: 2846-2856. DOI: 10.1016/j.enconman.2010.06.022

Delgado-Torres, A.M. and L. García-Rodríguez, 2010b. Preliminary design of seawater and brackish water reverse osmosis desalination systems driven by low-temperature solar Organic Rankine Cycles (ORC). Energy Convers. Manage., 51: 2913-2920. DOI: 10.1016/j.enconman.2010.06.032

Gang, P., L. Jing and J. Jie, 2011. Design and analysis of a novel low-temperature solar thermal electric system with two-stage collectors and heat storage units. Renewable Energy, 36: 2324-2333. DOI: 10.1016/j.renene.2011.02.008

He, Y.L., D.H. Mei, W.Q. Tao, W.W. Yang and H.L. Liu, 2012. Simulation of the parabolic trough solar energy generation system with Organic Rankine Cycle. Applied Energy, 97: 630-641. DOI: 10.1016/j.apenergy.2012.02.047

Hoffschmidt, B., S. Alexopoulos, C. Rau, J. Sattler and A. Anthrakidis *et al*., 2012. 3.18-Concentrating solar power. Comprehensive Renewable Energy.

Hung, T., S. Wang, C. Kuo, B. Pei and K. Tsai, 2010. A study of organic working fluids on system efficiency of an ORC using low-grade energy sources. Energy, 35: 1403-1411. DOI: 10.1016/j.energy.2009.11.025

ITW, 2012. Test report n. ITW, 11COL1028.

Kane, M., D. Larrain, D. Favrat and Y. Allani, 2003. Small hybrid solar power system. Energy, 28: 1427-1443. DOI: 10.1016/S0360-5442(03)00127-0

Klein, S.A., 2006. Solar energy laboratory, TRNSYS. A transient system simulation program. University of Wisconsin, Madison.

Kosmadakis, G., D. Manolakos and G. Papadakis, 2011. Simulation and economic analysis of a CPV/thermal system coupled with an organic Rankine cycle for increased power generation. Solar Energy, 85: 308-324. DOI: 10.1016/j.solener.2010.11.019

Ksayer, E.B.L., 2011. Design of an ORC system operating with solar heat and producing sanitary hot water. Energy Proc., 6: 389-395. DOI: 10.1016/j.egypro.2011.05.045

Kuo, C., S. Hsu, K. Chang and C. Wang, 2011. Analysis of a 50 kW organic Rankine cycle system. Energy, 36: 5877-5885. DOI: 10.1016/j.energy.2011.08.035

Li, C., G. Kosmadakis, D. Manolakos, E. Stefanakos and G. Papadakis *et al*., 2013. Performance investigation of concentrating solar collectors coupled with a transcritical organic Rankine cycle for power and seawater desalination co-generation. Desalination, 318: 107-117. DOI: 10.1016/j.desal.2013.03.026

Madhawa Hettiarachchi, H.D., M. Golubovic, W.M. Worek and Y. Ikegami, 2007. Optimum design criteria for an Organic Rankine cycle using low-temperature geothermal heat sources. Energy, 32: 1698-1706. DOI: 10.1016/j.energy.2007.01.005

Palmieri, V., C. Russo, E.A. Palmieri, S. Pezzullo and A. Celentano, 2009. Changes in components of left ventricular mechanics under selective beta-1 blockade: Insight from traditional and new technologies in echocardiography. Eur. J. Echocardiogr., 10: 745-52.
DOI: 10.1093/ejechocard/jep055

Pikra, G., A. Salim, B. Prawara, A.J. Purwanto and T. Admono *et al*., 2013. Development of small scale concentrated solar power plant using organic rankine cycle for isolated region in Indonesia. Energy Procedia, 32: 122-128.
DOI: 10.1016/j.egypro.2013.05.016

Quoilin, S., M. Orosz, H. Hemond and V. Lemort, 2011. Performance and design optimization of a low-cost solar organic Rankine cycle for remote power generation. Solar Energy, 85: 955-966.
DOI: 10.1016/j.solener.2011.02.010

Quoilin, S., M.V.D. Broek, S. Declaye, P. Dewallef and V. Lemort, 2013. Techno-economic survey of Organic Rankine Cycle (ORC) systems. 22: 168-186.
DOI: 10.1016/j.rser.2013.01.028

Rayegan, R. and Y.X. Tao, 2011. A procedure to select working fluids for Solar Organic Rankine Cycles (ORCs). Renewable Energy, 36: 659-670.
DOI: 10.1016/j.renene.2010.07.010

Saleh, B., G. Koglbauer, M. Wendland and J. Fischer, 2007. Working fluids for low-temperature organic Rankine cycles. Energy, 32: 1210-1221.
DOI: 10.1016/j.energy.2006.07.001

Tchanche, B., F.G. Lambrinos, A. Frangoudakis and G. Papadakis, 2011. Low-grade heat conversion into power using organic Rankine cycles-a review of various applications. Renewable Sustainable Energy Rev., 15: 3963-3979.
DOI: 10.1016/j.rser.2011.07.024

Tempesti, D. and D. Fiaschi, 2013. Thermo-economic assessment of a micro CHP system fuelled by geothermal and solar energy. Energy, 58: 45-51.
DOI: 10.1016/j.energy.2013.01.058

Tempesti, D., G. Manfrida and D. Fiaschi, 2012. Thermodynamic analysis of two micro CHP systems operating with geothermal and solar energy. Applied Energy, 97: 609-617.
DOI: 10.1016/j.apenergy.2012.02.012

Wang, M., J. Wang, Y. Zhao, P. Zhao and Y. Dai, 2013. Thermodynamic analysis and optimization of a solar-driven regenerative ORGANIC RANKINE CYCLE (ORC) based on flat-plate solar collectors. Applied Thermal Eng., 50: 816-825.
DOI: 10.1016/j.applthermaleng.2012.08.013

Yamamoto, T., T. Furuhata, N. Arai and K. Mori, 2001. Design and testing of the Organic Rankine Cycle. Energy, 26: 239-251.
DOI: 10.1016/S0360-5442(00)00063-3

Zhou, C., E. Doroodchi and B. Moghtaderi, 2013. An in-depth assessment of hybrid solar-geothermal power generation. Energy Convers. Manage., 74: 88-101.
DOI: 10.1016/j.enconman.2013.05.014